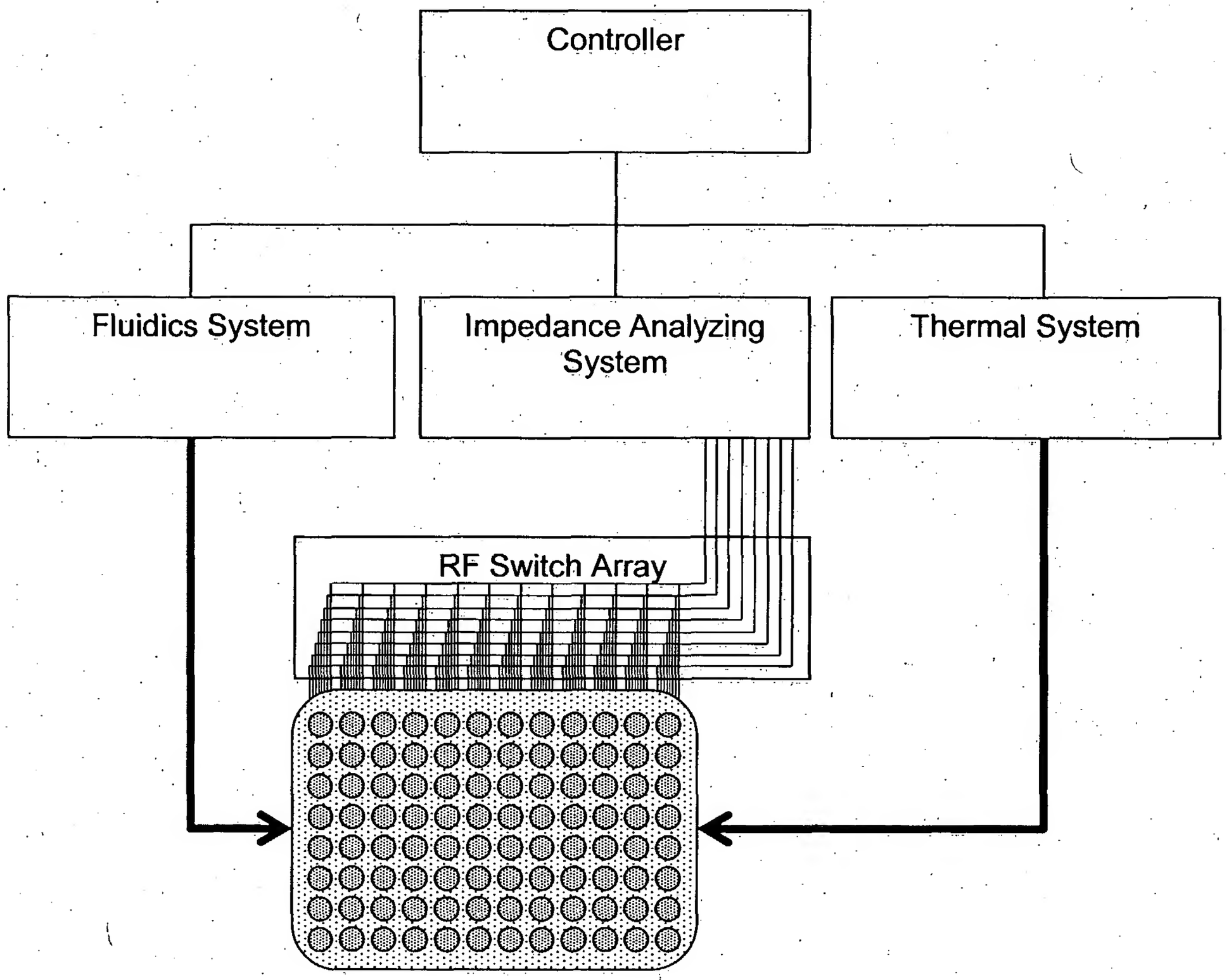

Figure 1a. A block diagram that illustrates one embodiment of the bioimpedance measuring system.

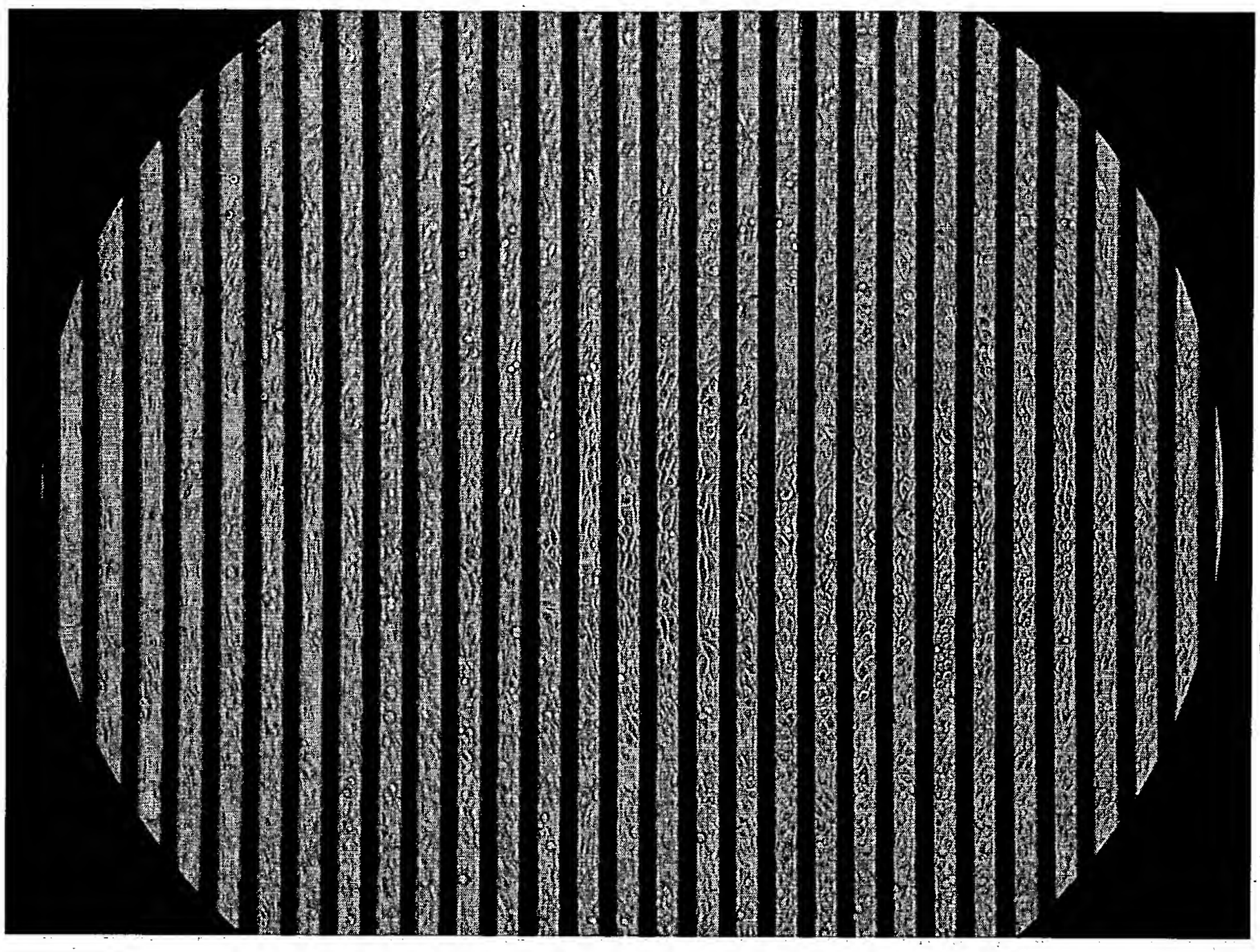

Figure 1b. The bioimpedance system displaying cells on the inter-digitated electrodes of a micro-titre plate well.

Figure 2

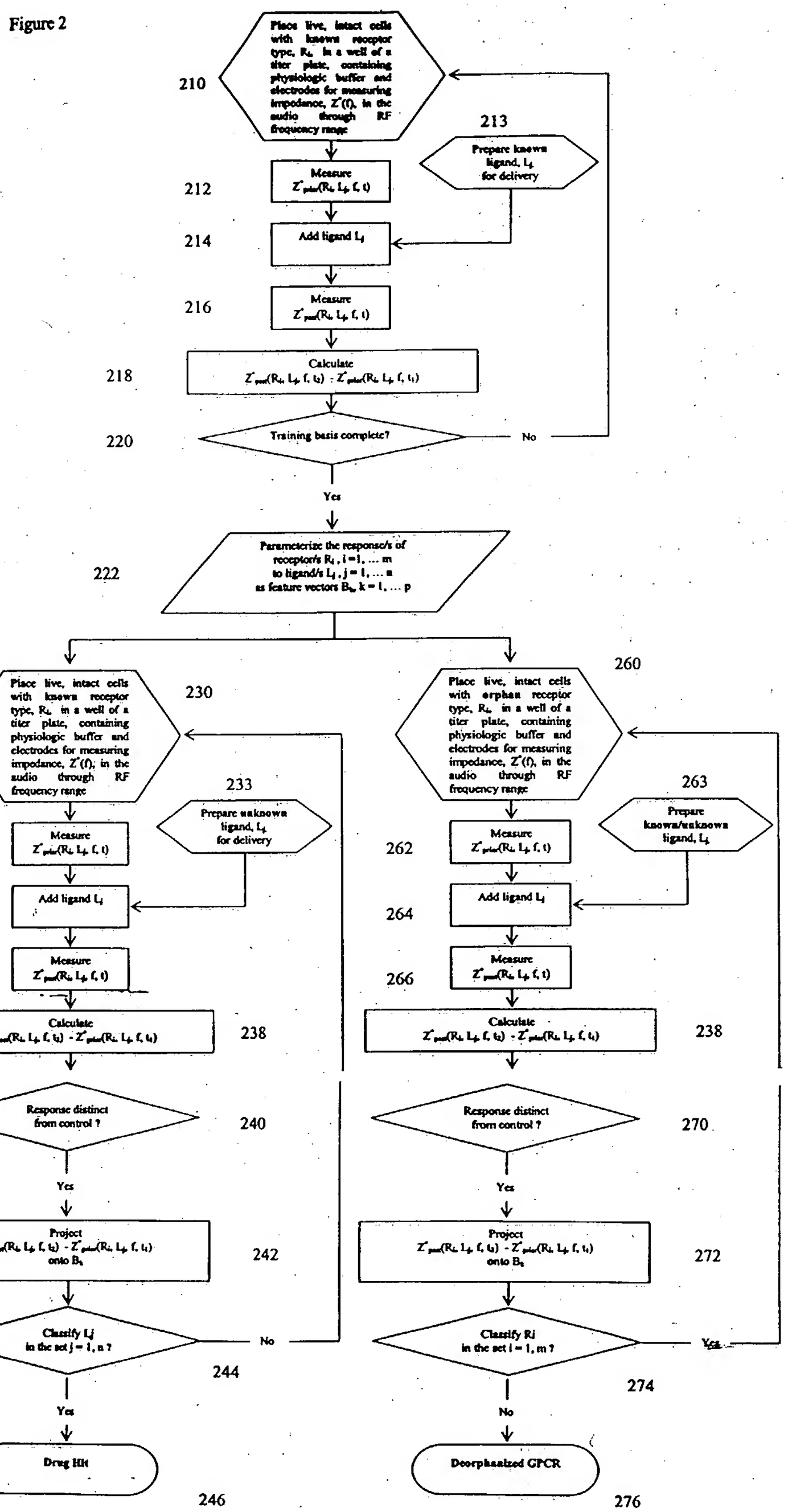
210
Place live, intact cells with known receptor type, R_i, in a well of a titer plate, containing physiologic buffer and electrodes for measuring impedance, $Z^*(f)$, in the audio through RF frequency range
213
Prepare known ligand, L_j for delivery
212
Measure $Z^*_{prior}(R_i, L_j, f, t)$
214
Add ligand L_j
216
Measure $Z^*_{post}(R_i, L_j, f, t)$
218
Calculate $Z^*_{post}(R_i, L_j, f, t_2) - Z^*_{prior}(R_i, L_j, f, t_1)$
220
Training basis complete?
No
Yes
222
Parameterize the response/s of receptor/s R_i, $i = 1, \ldots m$ to ligand/s L_j, $j = 1, \ldots n$ as feature vectors B_k, $k = 1, \ldots p$
230
Place live, intact cells with known receptor type, R_i, in a well of a titer plate, containing physiologic buffer and electrodes for measuring impedance, $Z^*(f)$, in the audio through RF frequency range
233
Prepare unknown ligand, L_j for delivery
232
Measure $Z^*_{prior}(R_i, L_j, f, t)$
234
Add ligand L_j
236
Measure $Z^*_{post}(R_i, L_j, f, t)$
238
Calculate $Z^*_{post}(R_i, L_j, f, t_2) - Z^*_{prior}(R_i, L_j, f, t_1)$
240
Response distinct from control ?
Yes
242
Project $Z^*_{post}(R_i, L_j, f, t_2) - Z^*_{prior}(R_i, L_j, f, t_1)$ onto B_k
244
Classify L_j in the set $j = 1, n$?
No
Yes
246
Drug Hit
260
Place live, intact cells with orphan receptor type, R_i, in a well of a titer plate, containing physiologic buffer and electrodes for measuring impedance, $Z^*(f)$, in the audio through RF frequency range
263
Prepare known/unknown ligand, L_j
262
Measure $Z^*_{prior}(R_i, L_j, f, t)$
264
Add ligand L_j
266
Measure $Z^*_{post}(R_i, L_j, f, t)$
238
Calculate $Z^*_{post}(R_i, L_j, f, t_2) - Z^*_{prior}(R_i, L_j, f, t_1)$
270
Response distinct from control ?
Yes
272
Project $Z^*_{post}(R_i, L_j, f, t_2) - Z^*_{prior}(R_i, L_j, f, t_1)$ onto B_k
274
Classify R_i in the set $i = 1, m$?
Yes
No
276
Deorphanized GPCR

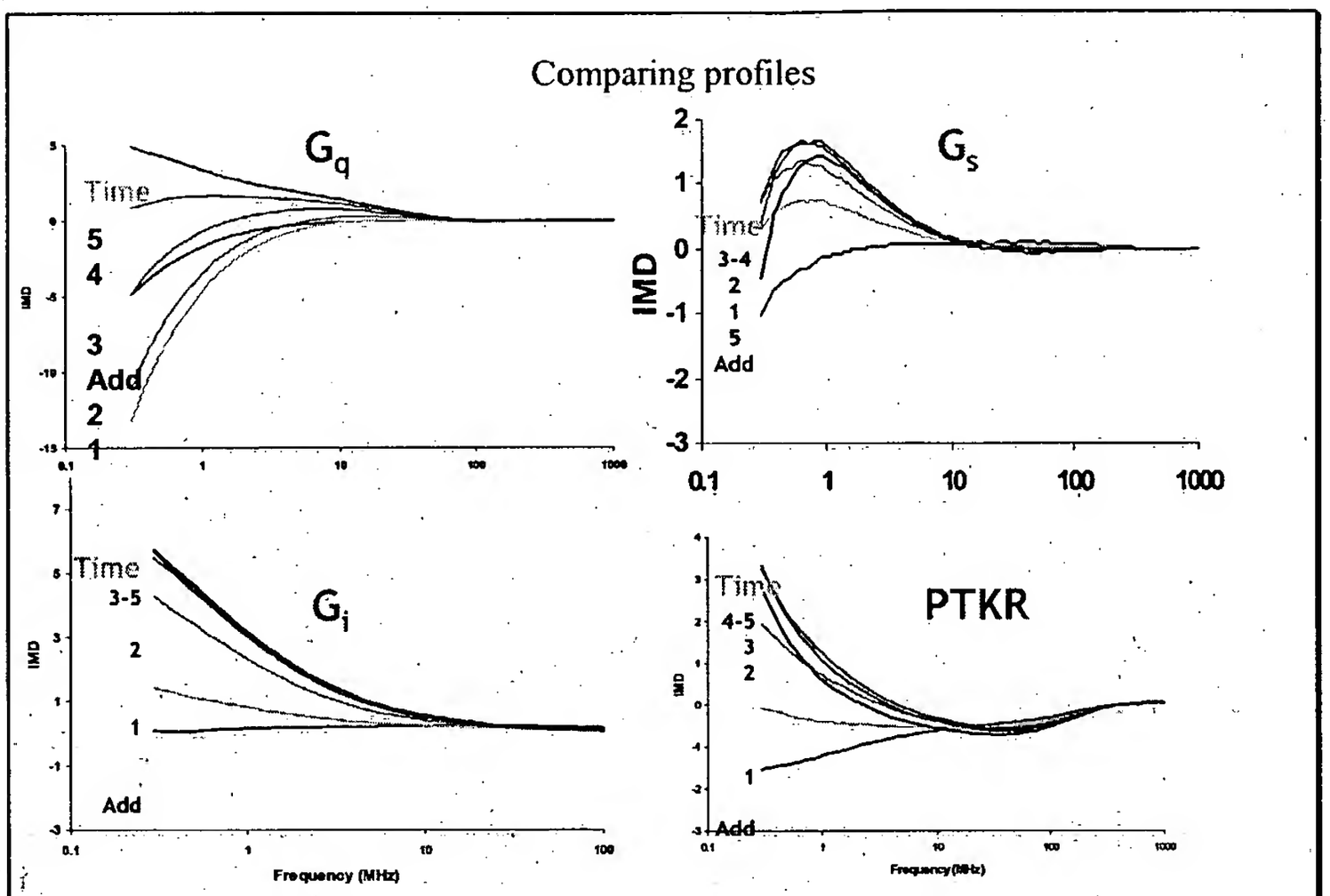

Figure 3. Raw impedance magnitude difference data for the four major receptor families studied.

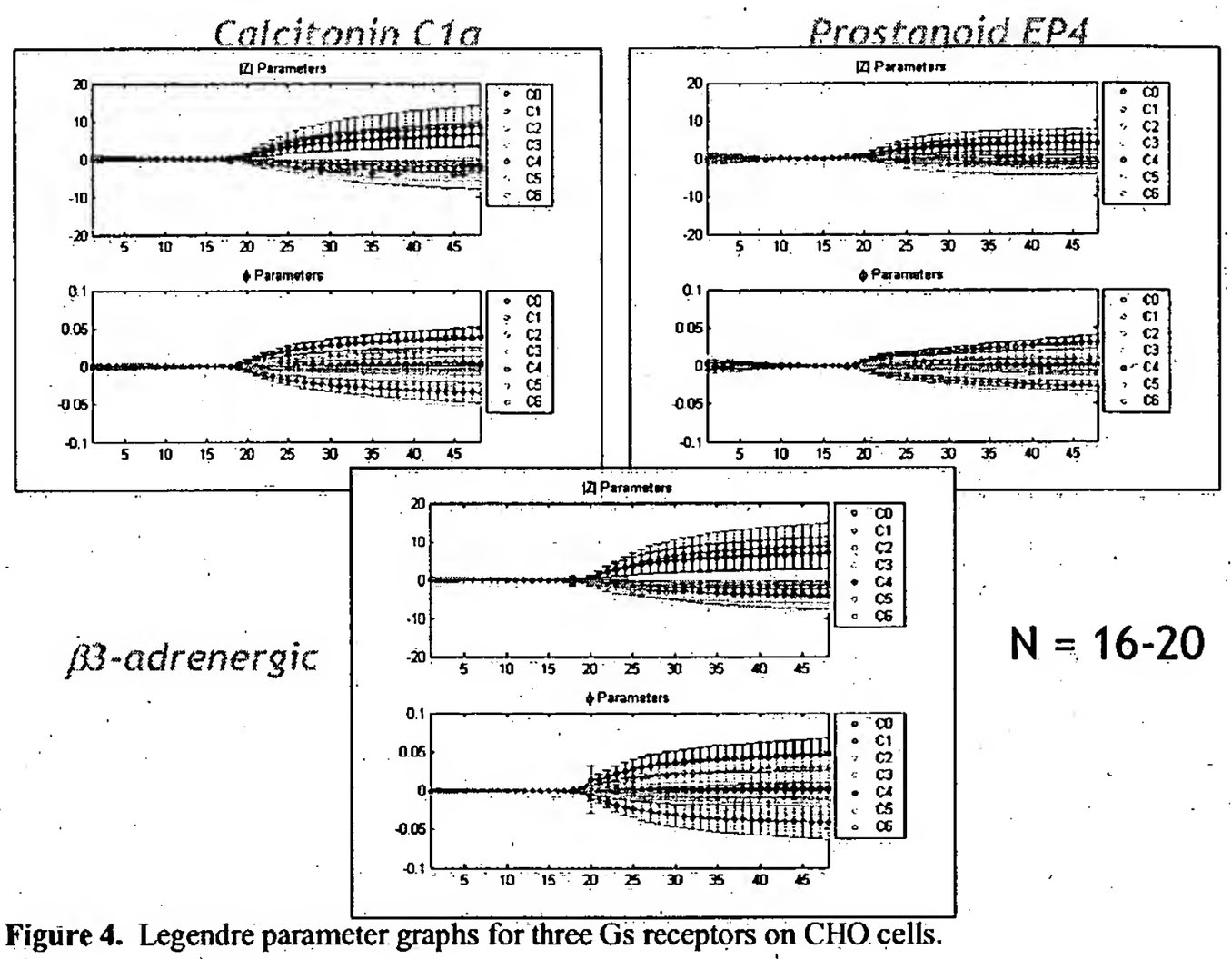

Figure 4. Legendre parameter graphs for three Gs receptors on CHO cells.

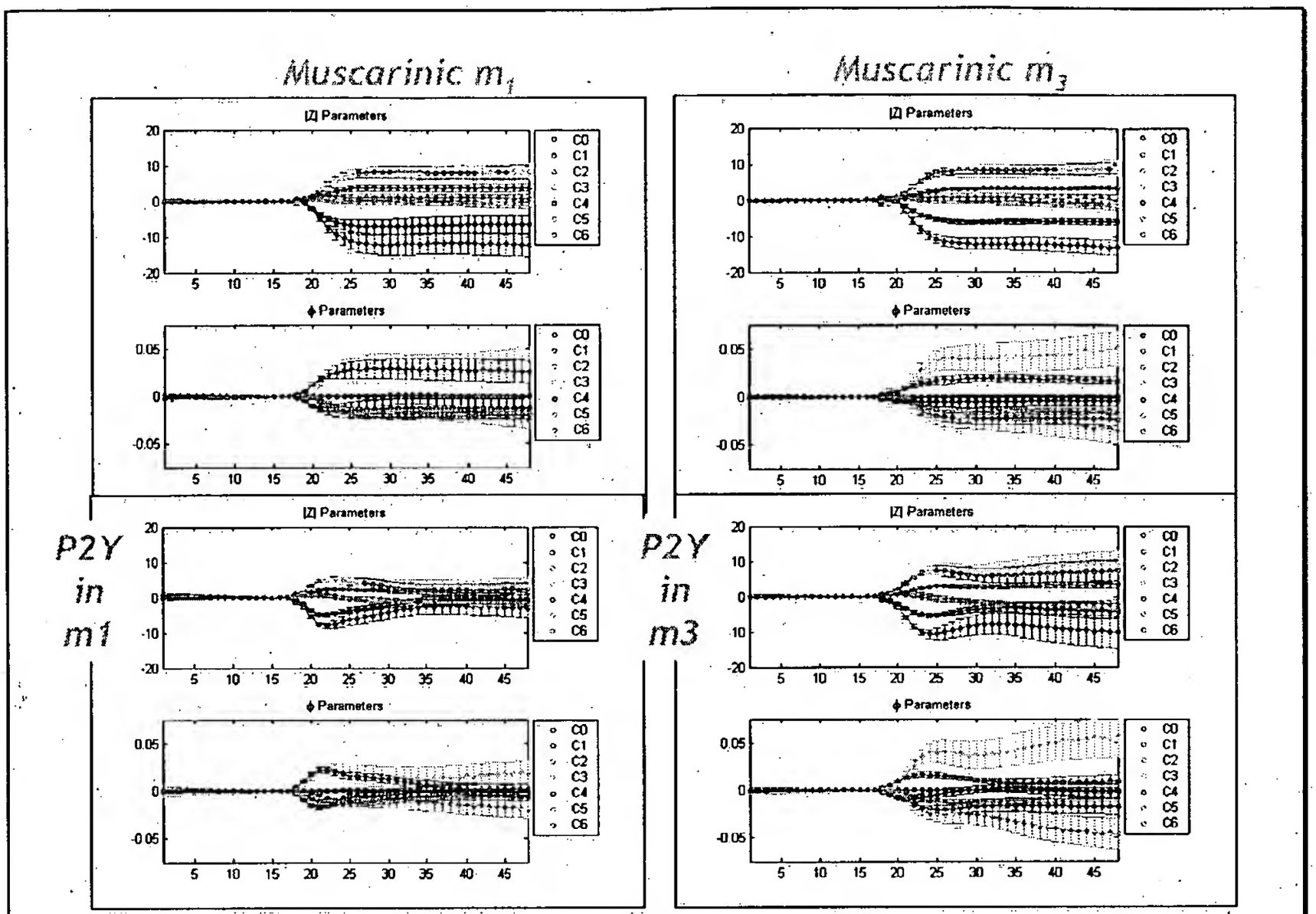

Figure 5. Legendre parameter graphs of three Gq receptors on CHO cells:

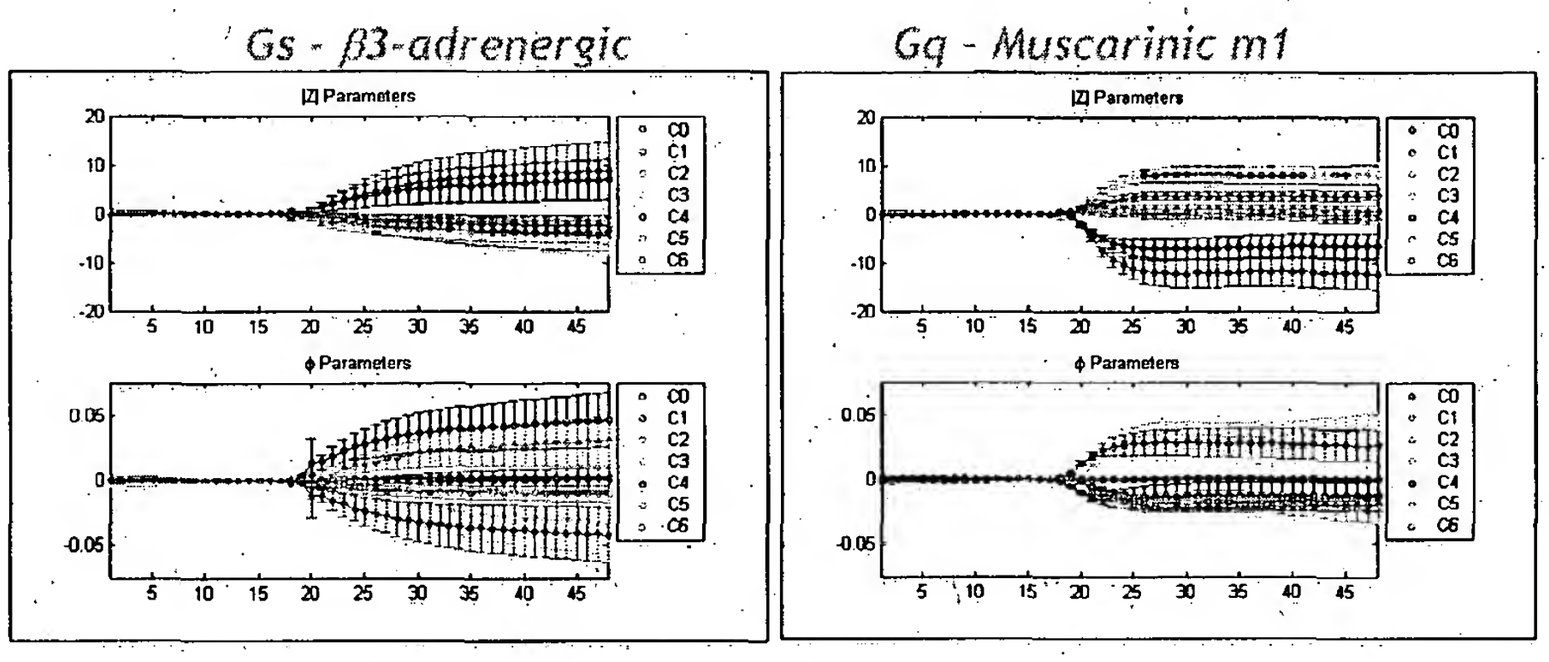

Figure 6. Comparison of parameter graphs for Gs and Gq receptors on CHO cells.

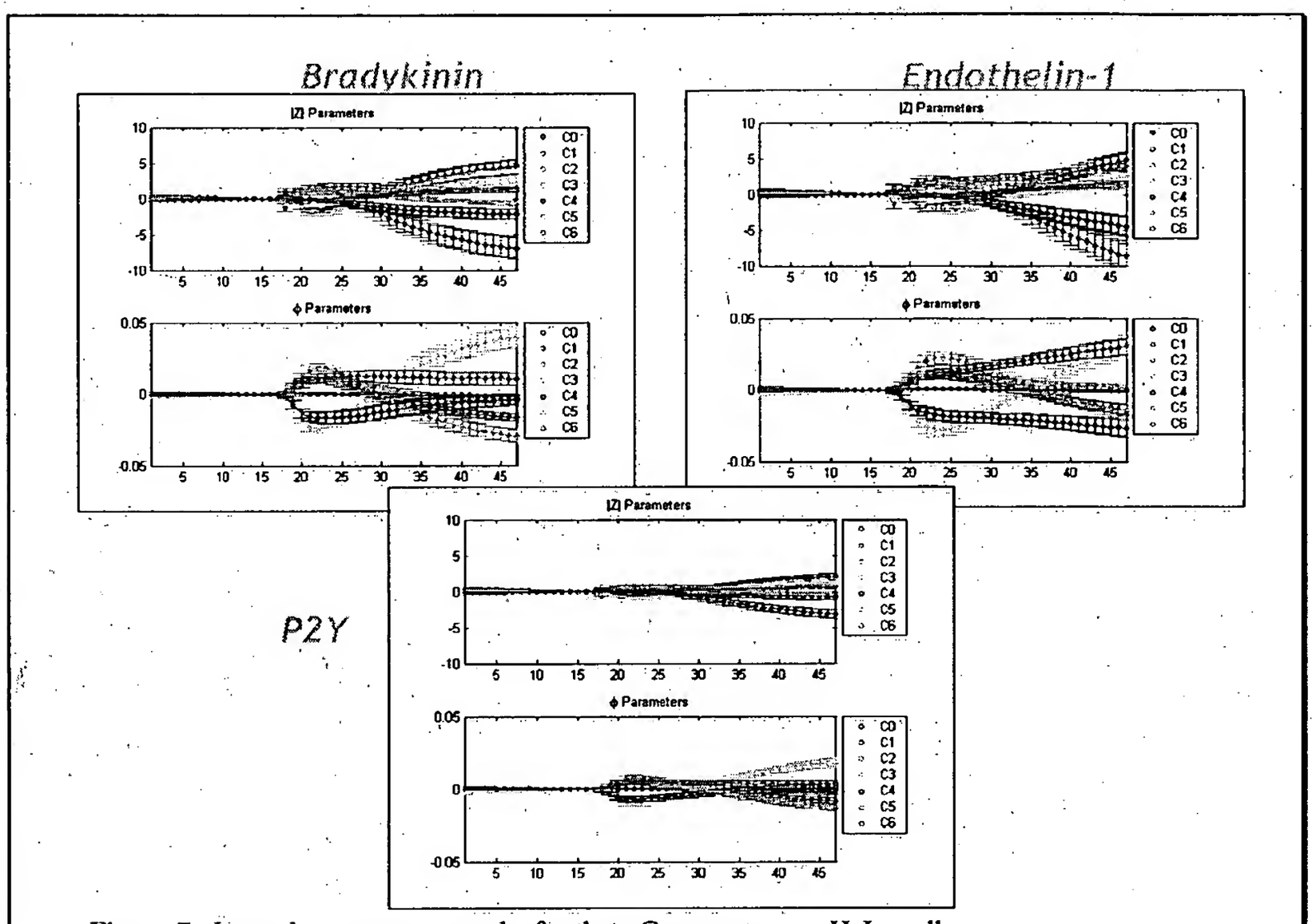

Figure 7. Legendre parameter graphs for three Gq receptors on HeLa cells.

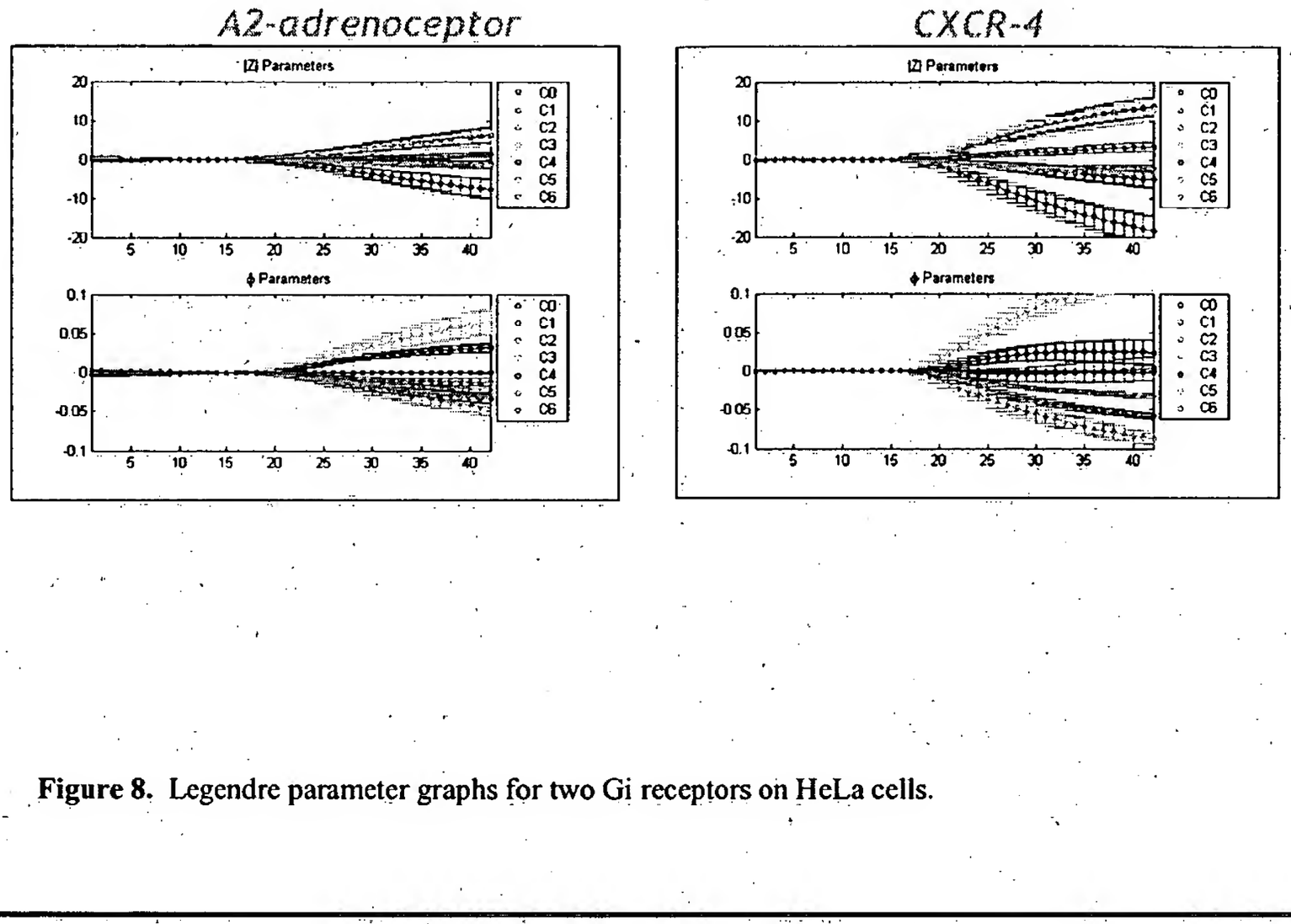

Figure 8. Legendre parameter graphs for two Gi receptors on HeLa cells.

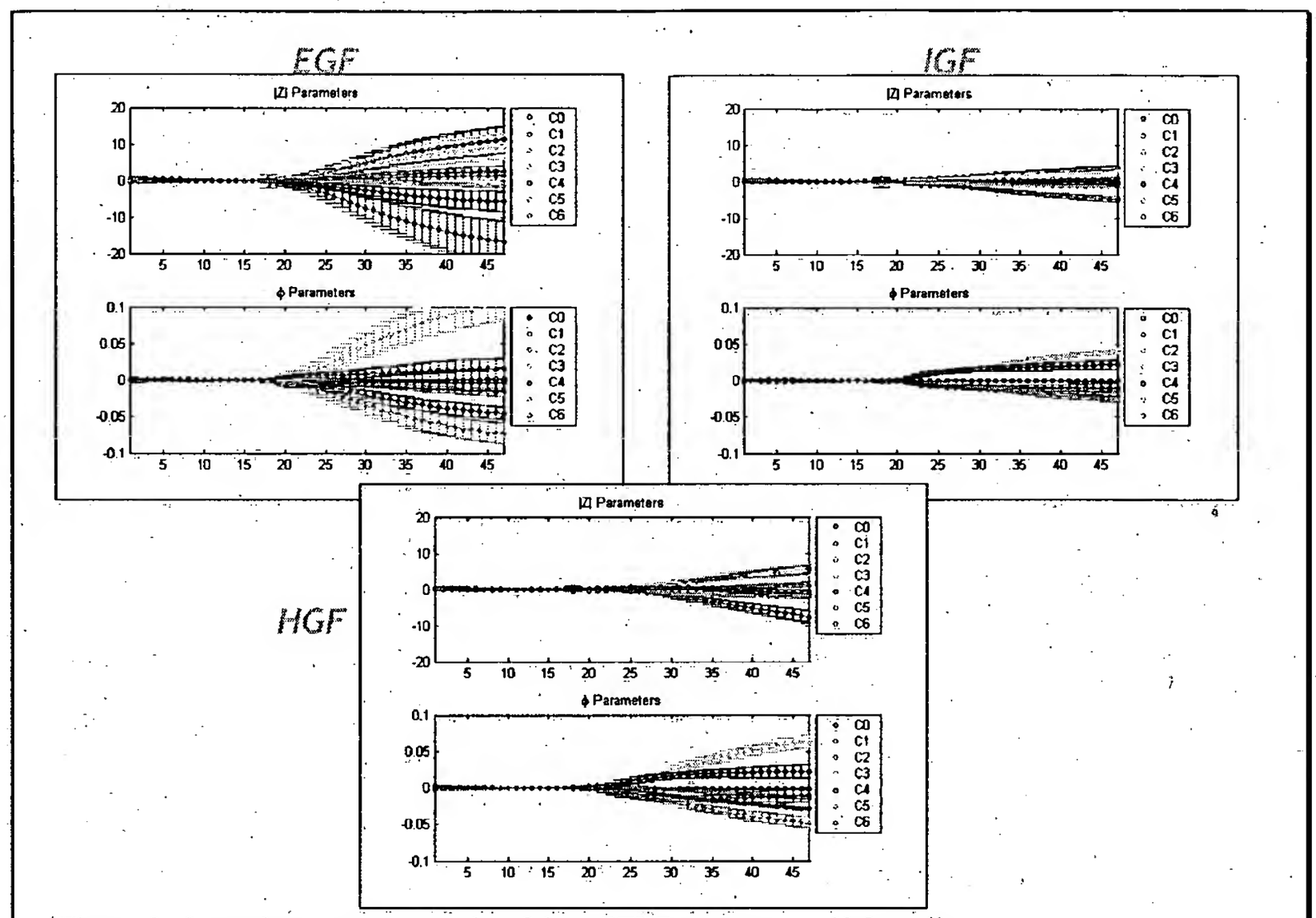

Figure 9. Legendre parameter graphs of three PTKR receptors on HeLa cells.

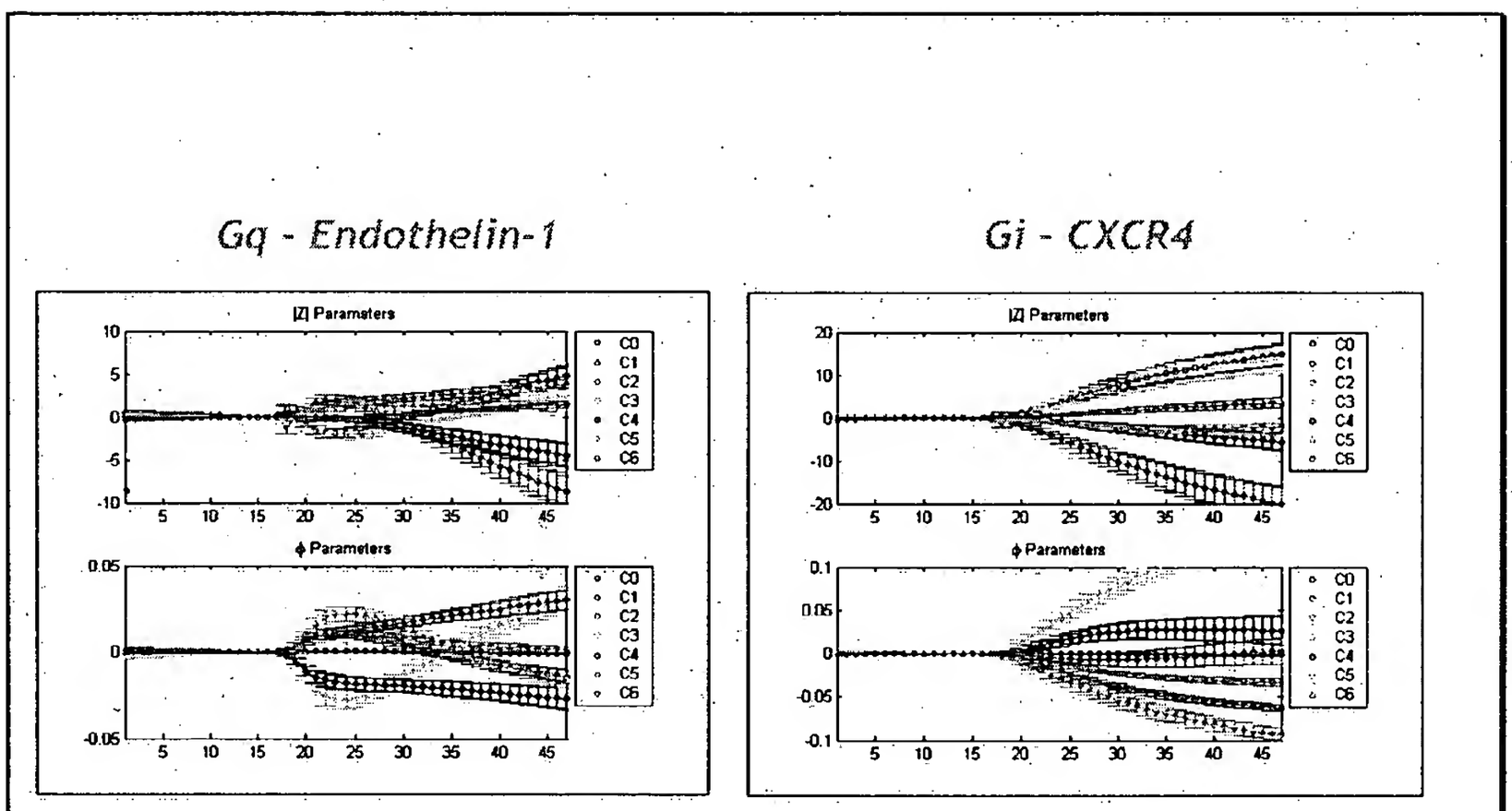

Figure 10. Comparison of parameter graphs for Gq and Gi receptors on HeLa cells.

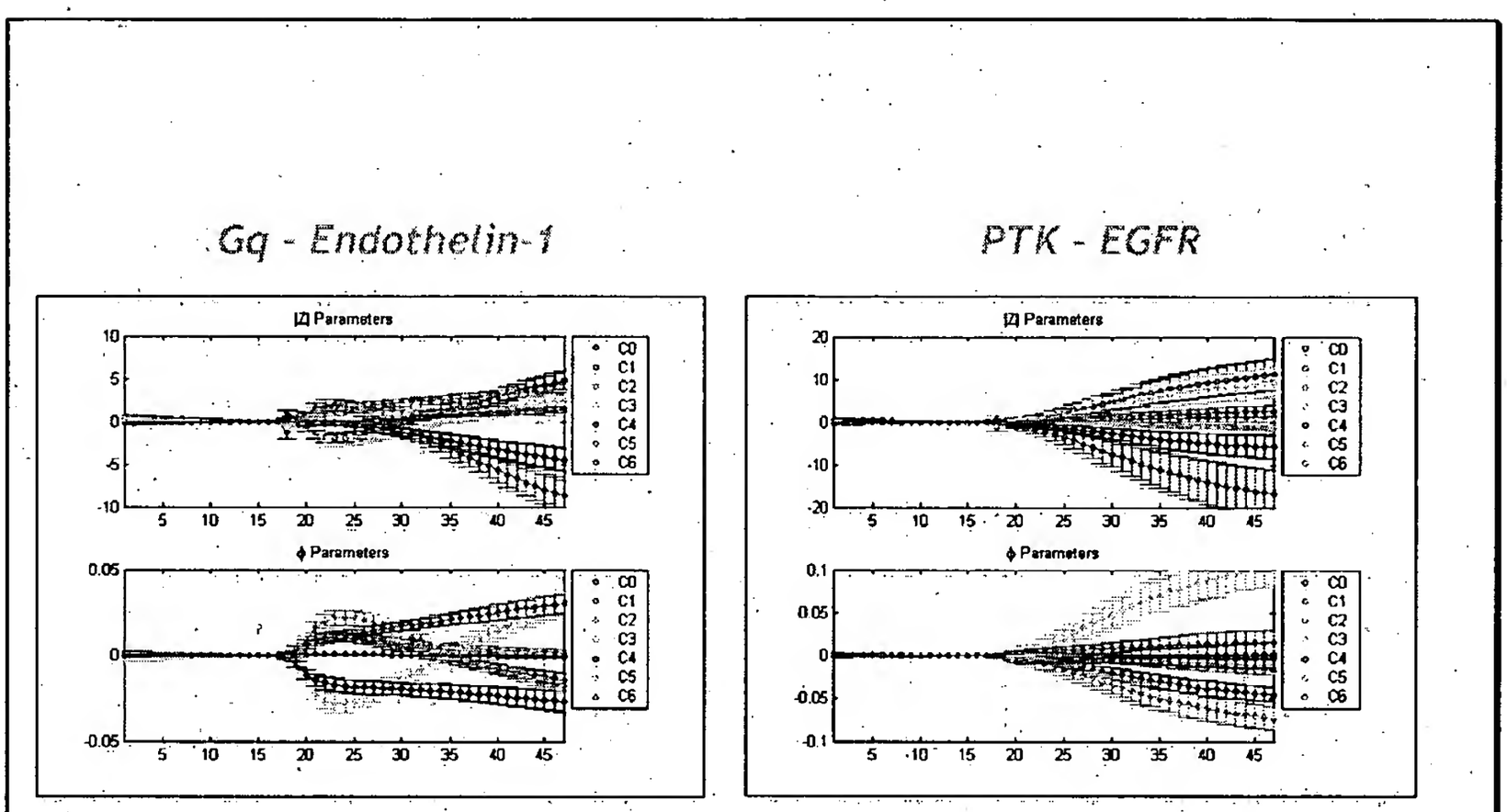

Figure 11. Comparison of parameter graphs for Gq and PTKR receptors on HeLa cells.

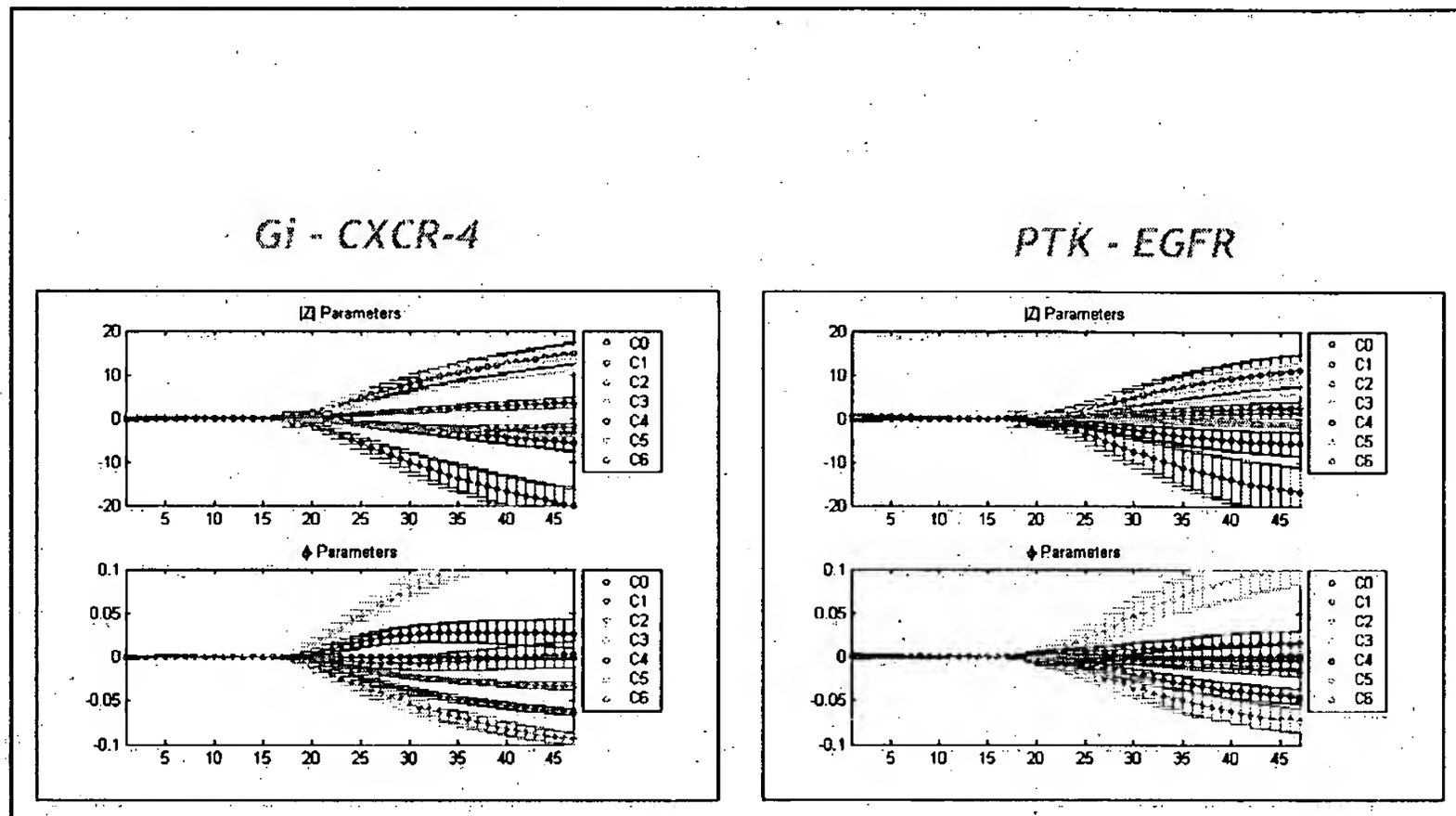

Figure 12. Comparison of parameter graphs for Gi and PTKR receptors on HeLa cells.

|Z| QDS		Predicted Membership				% error
		Buffer	Gq (m1)	Gs (β3)	Gi (k1)	
Actual Membership	Gq	0	77	0	0	0.0
	Gs	0	0	44	2	4.3
	Gi	0	3	0	33	8.3

total error
3.1 %

ϕ QDS		Predicted Membership				% error
		Buffer	Gq (m1)	Gs (β3)	Gi (k1)	
Actual Membership	Gq	0	77	0	0	0.0
	Gs	0	0	45	1	2.2
	Gi	0	7	2	27	25.0

total error
6.3 %

Figure 13. Analysis matrix showing results of standard multidimensional data classification using the confusion matrix technique on data from CHO cells.

|Z|		Predicted Membership				% error
Actual Membership		Buffer (SV)	Gi	Gq	PTK	
	Buffer (SV)	42	1	1	1	6.7
	Gi	0	46	0	0	0.0
	Gq	0	0	36	0	0.0
	PTK	3	1	0	37	9.8

total error
4.2 %

ϕ		Predicted Membership				% error
Actual Membership		Buffer (SV)	Gi	Gq	PTK	
	Buffer (SV)	40	0	1	4	11.1
	Gi	0	46	0	0	0.0
	Gq	0	0	36	0	0.0
	PTK	1	2	0	38	7.3

total error
4.8 %

Figure 14. Analysis matrix showing results of standard multidimensional data classification using the confusion matrix technique on data from HeLa cells.